Langmuir

Article

pubs.acs.org/Langmuir

# Adsorption Studies of *p*-Aminobenzoic Acid on the Anatase $TiO_2$(101) Surface

Andrew G. Thomas,*[,†] Mark J. Jackman,[†,‡] Michael Wagstaffe,[†,‡] Hanna Radtke,[‡] Karen Syres,[§] Johan Adell,[∥] Anna Lévy,[⊥] and Natalia Martsinovich[#]

[†]School of Materials and The Photon Science Institute and [‡]School of Physics and Astronomy, The University of Manchester, Oxford Road, Manchester M13 9PL, United Kingdom

[§]School of Chemistry, The University of Nottingham, University Park, Nottingham NG7 2RD, United Kingdom

[∥]MaxLab, Ole Römers väg 1, 223 63 Lund, Sweden

[⊥]Synchrotron Soleil, Orme des Merisiers, Saint Aubin, BP 48 - 91192 Gif-sur-Yvette, France

[#]Department of Chemistry, The University of Sheffield, Sheffield S3 7HF, United Kingdom

Supporting Information

**ABSTRACT:** The adsorption of *p*-aminobenzoic acid (pABA) on the anatase $TiO_2$(101) surface has been investigated using synchrotron radiation photoelectron spectroscopy, near edge X-ray absorption fine structure (NEXAFS) spectroscopy, and density functional theory (DFT). Photoelectron spectroscopy indicates that the molecule is adsorbed in a bidentate mode through the carboxyl group following deprotonation. NEXAFS spectroscopy and DFT calculations of the adsorption structures indicate the ordering of a monolayer of the amino acid on the surface with the plane of the ring in an almost upright orientation. The adsorption of pABA on nanoparticulate $TiO_2$ leads to a red shift of the optical absorption relative to bare $TiO_2$ nanoparticles. DFT and valence band photoelectron spectroscopy suggest that the shift is attributed to the presence of the highest occupied molecular orbitals in the $TiO_2$ band gap region and the presence of new molecularly derived states near the foot of the $TiO_2$ conduction band.

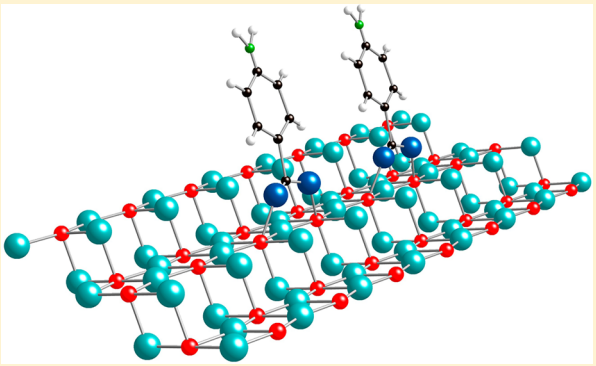

## 1. INTRODUCTION

The adsorption of organic molecules for the functionalization of titania is of interest for a number of technological applications including photovoltaics,[1] biosensors,[2] and targeted biomaterials to name but a few. The interaction of titania with amino acids in particular is interesting because it is well established that carboxylic acids bond strongly to titania surfaces in a bidentate bridging fashion, following the deprotonation of the acid group.[3,4] The adsorption of amino acids then has relevance in understanding surface interactions in novel biosensors based on $TiO_2$ and also in the osseointegration of Ti biomaterials, where the active surface is thought to be the native oxide.[5] The adsorption of amino acids on $TiO_2$ surfaces via the carboxyl group is thought to leave the amine group unbound.[6−8] The free amine group could then be used to graft polymers or biomolecules onto $TiO_2$ for biosensing[9] or novel biomaterial applications.[10] In addition, the free amine group could be used to anchor light-harvesting quantum dots, such as CdSe or PbS, to the $TiO_2$ surface.[11] The formation of a strong bond between the light-sensitizer and n-type material is thought to be important in allowing efficient charge transfer between the two materials in photovoltaics. Recently there have been a number of studies on CdSe and PbS quantum dots, which suggest that they exhibit multiple exciton generation, i.e., the production of more than one exciton for each absorbed photon. It has also been shown that charge transfer does occur between these quantum dots and $TiO_2$ single-crystal surfaces.[12] Cysteine linker molecules have been shown to enhance the efficiency of charge transfer between CdSe quantum dots and nanostructured $TiO_2$ surfaces relative to mercaptopropionic acid and thioglycolic acid linkers.[11] One might expect that an aromatic amino acid such as *p*-aminobenzoic acid (pABA) (Figure 1) may further enhance this effect because of the delocalization in the phenyl ring. The aromatic ring offers resonance structures for electron or hole trapping. This trapping, it has been suggested, can lead to an increase in the rate and efficiency of charge transfer when using cysteine as a linker molecule for CdSe quantum dots on nanostructured $TiO_2$ surfaces.[11]

Furthermore, pABA, like pyrocatechol (benzene-1,2-diol) and other catechols, causes an optical absorption shift when adsorbed onto $TiO_2$ nanoparticles, resulting in a color change

**Received:** August 16, 2014
**Revised:** September 23, 2014
**Published:** September 25, 2014

   dx.doi.org/10.1021/la5032619 | *Langmuir* 2014, 30, 12306−12314

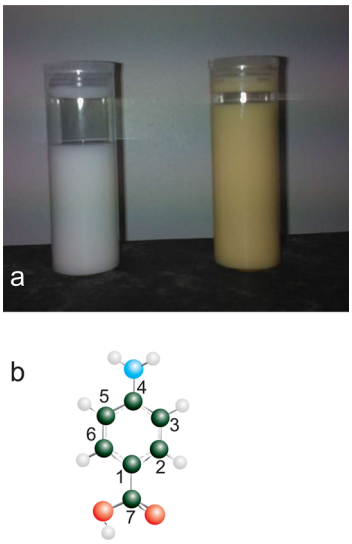


**Figure 1.** (a) Anatase $TiO_2$ nanoparticles suspended in water (left) and following the addition of *p*-aminobenzoic acid (right). (b) The pABA molecule. The numbering of the carbon atoms is used for reference below. Black/gray spheres represent C atoms, red spheres represent O atoms, blue spheres represent N atoms, and and white spheres represent H atoms.

from white to yellow (Figure 1a).[13,14] As in the case of catechol on $TiO_2$, this must be due to either a direct molecule to substrate $e^-$-transfer process[15] or a change in the density of states of the combined pABA-$TiO_2$ system because the optical absorption onset for pABA is 360 nm (3.4 eV).[16] The absorption onsets for anatase $TiO_2$ (3.2 eV) and pABA have led to their use in sunscreens.[13]

In this work, we study the adsorption mode and geometry of *p*-aminobenzoic acid on the anatase $TiO_2$(101) surface. The (101) surface is chosen because it is the lowest-energy surface of the common $TiO_2$ structures[17] and is therefore likely to be the most abundant surface in anatase powders. We also characterize the density of states of pABA adsorbed on single-crystal anatase $TiO_2$(101) in the valence band region using high-resolution valence band photoelectron spectroscopy in order to determine the nature of the change in the size of the optical gap seen in UV−visible absorption spectroscopy measurements. Finally, we utilize near-edge X-ray absorption fine structure (NEXAFS) spectroscopy to study the orientation of the pABA molecule on the anatase $TiO_2$(101) surface in order to verify that the amine group does not bond to the surface and is available for the grafting of other molecules or indeed quantum dots. DFT calculations are also used to study the interaction between pABA and the anatase $TiO_2$(101) surface, both to support the geometry investigations and to elucidate the optical absorption shift through the study of the density of occupied and unoccupied states.

## 2. EXPERIMENTAL AND COMPUTATIONAL DETAILS

Synchrotron radiation photoelectron spectra of clean- and pABA-dosed $TiO_2$ were recorded on the undulator beamline, I4, and bending-magnet beamline, D1011, at MAX-Lab, Sweden, and the undulator beamline, Antares, at Soleil, France. The anatase $TiO_2$(101) single crystal (Pikem Ltd.) was prepared by repeated 1 keV $Ar^+$ ion sputtering and 650 °C annealing cycles until sharp (1 × 1), low-energy electron diffraction (LEED) patterns were obtained. A survey photoelectron spectrum showed the surface to be free of contaminants. Two dosing methods were used. In the first method, pABA (99.9%, Sigma-Aldrich) was packed into a Ta envelope and thoroughly outgassed in an isolated chamber at 60 °C. The evaporator temperature was then reduced to 30 °C, and the sample was introduced into the dosing chamber and dosed for up to 30 min. The base pressure of the dosing chamber was kept below $5 \times 10^{-8}$ mbar, and the sample was kept under vacuum between dosing and data acquisition. This was determined to be saturation coverage because further exposure under these dosing conditions led to no increase in the size of the O 1s photoemission peak associated with the adsorption. Comparison with O 1s spectra following the adsorption of similar molecules on this surface also supported this coverage.[18] The second method involved pABA being placed in a sealed, evacuated port at room temperature behind a leak valve. Dosing was performed by opening the valve, which for an exposure of 10 L (1 L = $1.33 \times 10^{-6}$ mbar s) and by a comparison of O 1s spectra with the first method also resulted in approximately 1 ML of coverage. In both cases, the sample was at room temperature throughout the dosing and measurements.

Photoelectron spectra were recorded at normal emission and are aligned on the binding-energy scale referenced to a Fermi edge spectrum recorded from the Ta clips holding the sample in place, unless otherwise stated. NEXAFS spectra were recorded on beamline D1011 at MAX-Lab using a partial yield detector. The photon energy was scanned over the C K-edge monitoring all photoemitted electrons with a kinetic energy of ≥250 eV. The sample was oriented such that the electric vector was aligned at 17° relative to the [010] azimuth. NEXAFS spectra were recorded at 10° polar angle intervals from normal incidence up to 70° from normal incidence. Spectra were divided by the spectrum recorded from the clean surface to remove any substrate-related features from the spectra. Spectra are aligned on the photon energy scale relative to the Ti L edge at 458.4 eV.[19]

To compare the adsorption of pABA on $TiO_2$ via the carboxylic group or via both the carboxylic and the amino group, several adsorption configurations of pABA on $TiO_2$ anatase (101) slabs were modeled using density-functional theory (DFT) calculations. The calculations were performed using the CRYSTAL09 code[20,21] and employed the all-electron representation with localized Gaussian basis sets (triple valence plus polarization for Ti and O and double valence plus polarization for N, C, and H, all obtained from the CRYSTAL web site[22]) and the B3LYP hybrid density functional.[23,24] This setup was tested in an earlier publication.[25] Periodic $TiO_2$ slabs were modeled using the 2D option in CRYSTAL and contained two $Ti_2O_4$ layers (12 atomic layers) and (3 × 3) extended surface unit cells. Atoms in the lower half of the slab were fixed at their bulk positions, and the upper half of the slab and the adsorbate were allowed to relax. These (3 × 3) extended cells were large enough to ensure no interaction between adsorbate molecules in periodically repeated image cells. Thus, these calculations represented isolated adsorbate molecules rather than a monolayer. Following literature studies of carboxylic acids, such as formic acid,[26,27] benzoic acid,[25] and other aromatic carboxylic acids[4] on the anatase (101) surface, two modes of adsorption of the carboxylic group were considered: dissociative adsorption in the bridging bidentate configuration and nondissociative (molecular) adsorption. Additionally, for each of these adsorption modes of the carboxylic group, adsorption configurations were constructed where the amino group was also interacting with the anatase (101) surface.

Adsorption energies $E_{ads}$ of optimized structures were calculated as

$$E_{ads} = E_{slab+ads} - E_{slab} - E_{pABA} \quad (1)$$

where, $E_{slab}$ is the energy of the $TiO_2$ slab, $E_{pABA}$ is the energy of the isolated pABA molecule in the gas phase, and $E_{slab+ads}$ is the energy of the surface-adsorbate system. Negative values of adsorption energies correspond to favorable adsorption. Adsorption energies were corrected for the basis set superposition error (BSSE) using the counterpoise scheme.[28]

To calculate NEXAFS spectra of the gas-phase pABA molecule, we used GaussView and Gaussian 03[29] to produce energy-minimized geometry-optimized structures in order to obtain the atomic coordinates. These calculations were carried out using DFT B3LYP


dx.doi.org/10.1021/la5032619 | *Langmuir* 2014, 30, 12306−12314

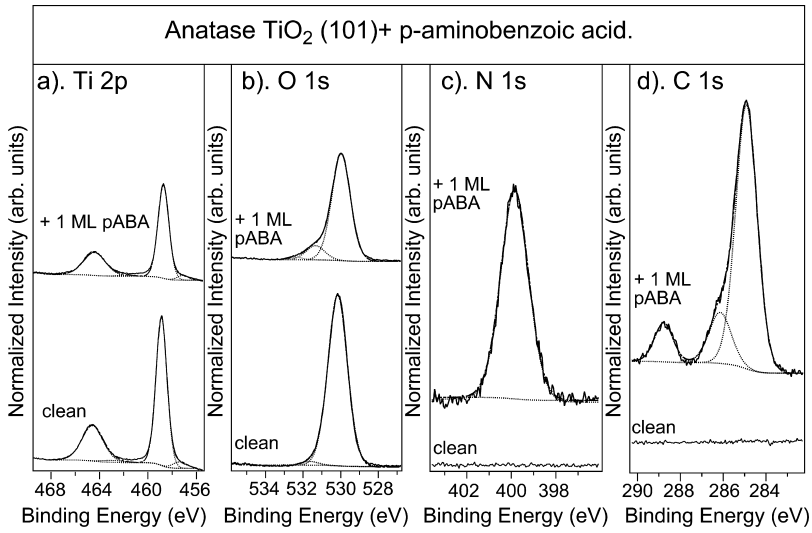


**Figure 2.** Core-level synchrotron radiation photoemission spectra of a clean anatase $TiO_2(101)$ single crystal and the anatase $TiO_2(101)$ single crystal following the adsorption of ~1 ML of pABA. (a) Ti 2p, (b) O 1s, (c) N 1s, and (d) C 1s.

theory and the 6-31G(d,p) basis set. The coordinates obtained from Gaussian were then used to carry out further DFT calculations using the StoBe-deMon code.[30] StoBe was used to calculate the excited-state X-ray absorption spectra for each C atom in the molecule individually. The summation of the individual energy-calibrated spectra gives the theoretical angle-integrated NEXAFS spectrum for the molecule.

## 3. RESULTS AND DISCUSSION

**3.1. Photoelectron Spectroscopy.** Figure 2 shows the Ti 2p, O 1s, N 1s, and C 1s photoelectron spectra recorded from clean anatase $TiO_2(101)$ and anatase $TiO_2(101)$ following the adsorption of a monolayer (1 ML) of pABA at a photon energy ($h\nu$) of 1000 eV. These spectra were recorded on bending magnet beamline D1011. We define 1 ML in this case as saturation coverage, where all available 5-fold-coordinated Ti sites on the surface are occupied. The coverage is monitored from the relative intensity of the molecule-to-substrate O 1s signal.[31] Figure 2a shows the Ti 2p spectra, which consist of two peaks due to spin−orbit splitting: the Ti $2p_{3/2}$ peak at a binding energy of 458.9 eV and the Ti $2p_{1/2}$ peak at 464.5 eV. The small peak at a binding energy of 457.4 eV is evidence of residual $Ti^{3+}$, which for anatase $TiO_2(101)$ is thought to arise from subsurface oxygen vacancies[32] or possibly from step edges on the (101) surface.[33] Following exposure to pABA, the Ti 2p spectrum shows no significant change apart from a rigid shift of 0.2 eV to lower binding energy, which is also observed in the O 1s spectra in Figure 2b, and a small reduction in the intensity of the $Ti^{3+}$-derived peak. The shift is due to adsorbate-induced upward band bending and has been observed following the adsorption of other molecules on the $TiO_2$ anatase surface.[18,34] The reduction in the intensity of the $Ti^{3+}$-derived peak in the Ti 2p spectrum may suggest some degree of reoxidation of surface $Ti^{3+}$ upon adsorption of the amino acid, as has been observed following the adsorption of similar molecules.[34] However, it is also possible that the reduction in the intensity of the $Ti^{3+}$ peak in the Ti 2p spectrum relative to the $Ti^{4+}$ peak is due to preferential adsorption of the molecule at O-vacancy sites, where $Ti^{3+}$ is located.

Figure 2b shows the O 1s spectrum recorded from the clean $TiO_2$ anatase (101) surface ($h\nu$ = 1000 eV) fitted with two peaks at binding energies of 530.2 and 531.5 eV, which are assigned to the oxide and surface oxygen close to O-vacancy sites,[35,36] respectively. It is also possible that the higher energy peak arises from adsorbed hydroxyls[37] or from step edges.[33] Following the adsorption of around 1 ML of pABA onto the $TiO_2$ surface, the shoulder on the high-binding-energy side of the "oxide peak" is seen to increase in intensity. The O 1s spectrum can be fitted with two peaks at energies of 530.0 and 531.3 eV. By comparison with the adsorption of similar molecules on $TiO_2$ surfaces,[38−40] we assign the peak at 530.0 eV to the oxide substrate peak and that at 531.3 eV to the $COO^-$ moiety of the amino acid. Following the adsorption of pABA on the $TiO_2(101)$ surface, there is only a single O 1s peak associated with the molecule, strongly suggesting adsorption through both oxygen atoms in the carboxyl group following the loss of the proton from the carboxylic acid group.[39] If the carboxyl group had remained intact, then one would expect a second adsorbate-derived peak at higher binding energy to be present because of the chemically shifted C−OH group.[39] The dissociation of the carboxyl group, in conjunction with studies of adsorption of other carboxylic acids on $TiO_2$ surfaces,[40] suggests that the molecule adsorbs dissociatively on anatase $TiO_2$ in a bidentate configuration via the carboxylate group. From the data here it is not possible to determine unambiguously whether this is a chelating or bridge-bonding mode. However, previous studies on the adsorption of carboxylic acids on anatase and rutile $TiO_2$ surfaces seem to show a preference for the bidentate bridging mode.[4,40]

The N 1s spectrum following the adsorption of 1 ML pABA on the $TiO_2$ anatase surface is shown in Figure 2c. The spectrum consists of a single peak at a binding energy of 399.9 eV consistent with the presence of $NH_2$.[8,18,41] This suggests that the molecule does not form the zwitterion upon adsorption, in agreement with the adsorption of glycine on rutile $TiO_2(011)$;[8] therefore, it appears that the amine group is present as R−$NH_2$. This may suggest that the proton lost from the carboxylate group is adsorbed on the surface to form a surface hydroxyl species, as has been observed in other carboxylic acids upon adsorption on $TiO_2$ surfaces.[4]

The C 1s spectrum recorded following the adsorption of pABA on the anatase $TiO_2(101)$ surface is also shown in Figure 2d, indicating the presence of three peaks at energies of 284.9, 286.2, and 288.4 eV. These are assigned to carbon atoms C1−3


dx.doi.org/10.1021/la5032619 | Langmuir 2014, 30, 12306−12314

and C5−6 (284.9 eV), C4 (286.2 eV), and C7 (288.4 eV), where C1−C7 refers to the numbering in Figure 1b. The ratio of the C 1s peak areas for the adsorbed pABA molecule is found to be 8.1:1.6:1.0. Deviations from the expected stoichiometry in similar adsorbed molecules such as this have been explained as being due to photoelectron diffraction effects,[42] where the ordering of the overlayer and the substrate means that atoms at particular positions lead to the diffraction of the photoemitted electrons and in turn a reduction in the intensity of signals from electrons of a particular kinetic energy. In fact, the ring carbon/C−$NH_2$ ratio of 5.2:1 is in reasonable agreement with the expected ratios for this molecule. A reduction in intensity of the carboxyl-carbon-derived peak is consistent with bonding to the surface via the carboxylate group because emission from the carbon atom closest to the surface would be most susceptible to diffraction effects. Unfortunately, the sample manipulator used on D1011 did not allow azimuthal rotation, and energy scanned mode photoelectron diffraction measurements were not made so it is not possible to confirm that the effect is due to photoelectron diffraction. The discrepancy between the measured and expected peak ratios may of course arise from photon-beam-induced decomposition of the molecules with the loss of CO or $CO_2$ from the surface. However, no changes in the relative intensities of the C 1s peaks (or O 1s) were observed over time scales of several hours under the beam.

**3.2. Near-Edge X-ray Absorption Fine Structure (NEXAFS).** To probe the unoccupied molecular states, we carried out NEXAFS of the pABA powder and a 1 ML coverage of pABA on anatase $TiO_2$(101). The spectra recorded from the pABA powder and from 1 ML of adsorbed pABA with the incident synchrotron beam at 45° and 40° off normal incidence, respectively, are shown in Figure 3. The 1 ML spectrum is normalized by dividing by a spectrum recorded from the clean anatase $TiO_2$(101) surface and that from the powder by dividing by the photon flux over the energy range of the spectrum. The large dips in both sets of experimental spectra at around 290−295 eV arise from C contamination of the beamline optics, resulting in absorption at these energies. It is also noted that the 1 ML pABA-$TiO_2$ spectrum was recorded using a partial yield detector with a kinetic energy cut off of 250 eV on the D1011 bending magnet beamline. The spectrum from the pABA powder was recorded in constant final state mode using the Scienta analyzer to detect C KLL Auger electrons at 260 eV on insertion device beamline ANTARES at Soleil. The large dip at around 290 eV photon energy is an artifact of the beamline. The experimental NEXAFS spectra are in good agreement with those reported by Lopez et al. for the adsorption of pABA on Na-modified Si(100) 2 × 1 surfaces.[43] Figure 3 also shows the StoBe-calculated NEXAFS spectrum for the pABA molecule. The X-ray absorption spectra at the C K-edge are calculated for each atom individually, and each spectrum is energy calibrated and convoluted with a Gaussian distribution to give a similar peak width to the experimental data before summation to give the total spectrum for the molecule. The spectra for the individual C atoms are shown in the right-hand panel of Figure 3. Numbering C1−C7 refers to the schematic of the molecule in Figure 1 and can be used to assign the origin of the peaks seen in the experimental spectra.

The experimental and calculated spectra exhibit three clear shape resonances, at 284.5 eV, 285.9 eV and 287.8 eV in the powder and 284.5 eV, 285.8 eV and 287.7 eV in the monolayer spectrum, and 284.5 eV, 285.8 eV, and 287.4 eV for the

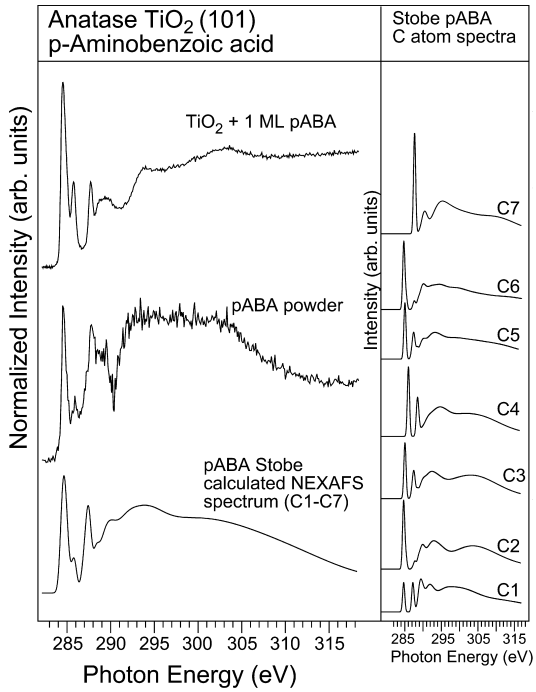


**Figure 3.** NEXAFS spectra recorded from pABA powder and 1 ML of pABA adsorbed on an anatase $TiO_2$(101) single crystal at normal emission compared to the angle-integrated StoBe-calculated NEXAFS spectrum. The panel on the right shows the individual contributions of the carbon atoms. Labels C1−C7 refer to the numbers in Figure 1b.

calculated spectrum. These sharp features are associated with excitations from C 1s → ring $\pi^*$ orbitals in the molecule. An analysis of the calculated spectra for the individual atoms, shown in Figure 3, indicate the three sharp resonances to be due to C $1s_{C-C} \rightarrow \pi^*_1$ (284.5 eV), C $1s_{C-N} \rightarrow \pi^*_1$ and C $1s_{C-C} \rightarrow \pi^*_3$ (285.8 eV), and C $1s_{C=O} \rightarrow \pi^*_1$ and C $1s_{C-N} \rightarrow \pi^*_3$ (287.8 eV) transitions, respectively.[43] In addition, a careful inspection of the lowest unoccupied molecular orbital (LUMO) peak shapes for C2 and C6 show some asymmetry. This is due to excitations from C 1s to the LUMO + 1 ($\pi^*_2$). The broad peaks above 290 eV photon energy are assigned to C 1s → $\sigma^*$ transitions.

Figure 4 shows angle-resolved NEXAFS of the 1 ML pABA on anatase $TiO_2$(101). The spectra are normalized to the absorption edge step.[44] The incident radiation is oriented with the electric vector at 17 ± 5° with respect to the [010] azimuth. It can be seen that at normal incidence the spectra are dominated by the $\pi^*$ peaks, but as we move to grazing incidence, the $\sigma^*$ peaks become larger with a concomitant decrease in the intensity of the $\pi^*$ peaks. The inset shows the intensity of the C $1s_{C-C} \rightarrow \pi^*_1$ transitions as a function of angle. The solid line is a fit based on the equations of Stöhr for a surface of 2-fold symmetry.[45] The fit is consistent with the molecule adsorbing with the plane of the ring tilted 30 ± 15° from the normal to the surface (60 ± 15° from the surface). The fit and Stöhr equations also give the azimuthal orientation and show the ring to lie at 24 ± 15° with respect to the direction of the electric vector. Because the synchrotron light was incident at 17° to the [010] azimuth, we calculate the ring to be aligned at an angle of 7 ± 15° relative to the [010] azimuth. Because of the sample manipulator having no azimuthal control, it was not possible to record NEXAFS spectra at differing azimuthal angles, and thus the error is large,


dx.doi.org/10.1021/la5032619 | Langmuir 2014, 30, 12306−12314

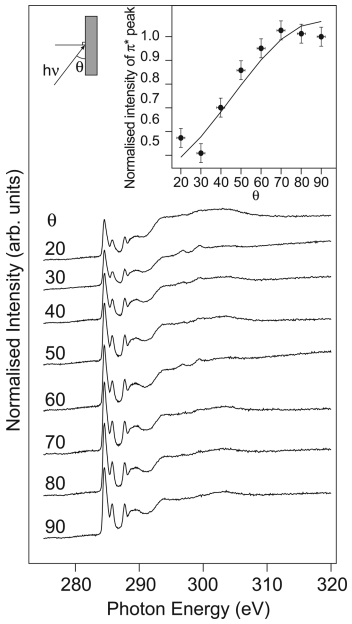


**Figure 4.** (a) Angle-resolved NEXAFS spectra recorded from the 1 ML pABA dosed anatase $TiO_2$(101) single crystal. $\theta$ is the angle of incident synchrotron radiation relative to the surface. The inset shows the intensity of the dominant $\pi^*$ peak as a function of angle. The line is a fit to the data using the equations of Stöhr.[46]

although it is clear that there is ordering of the adsorbed molecules.

**3.3. DFT Calculations.** Although the O 1s photoelectron spectroscopy data clearly point to a bidentate adsorption mode, which suggests deprotonation of the carboxyl group, and the NEXAFS spectroscopy suggests a tilt from an upright adsorption geometry, a number of groups have proposed that amino acids bond to $TiO_2$ surfaces through both the carboxylate and the amino groups.[46−48] Furthermore, the N 1s spectra tell us only that there is a single chemical environment for the amine nitrogen but do not exclude the possibility of the amine group interacting with the surface. To explore further whether the amino group is involved in the adsorption of pABA on anatase (101), DFT calculations were carried out. Several types of adsorption configurations were explored (Supporting Information). To obtain a comprehensive picture of the adsorption of pABA via the amino group, different orientations of the molecule with respect to the surface crystallographic directions were tested; the amino group was adsorbed either intact or dissociatively (losing one hydrogen). Because the number of reduced sites in the anatase sample used here is very small according to our experiments (very small $Ti^{3+}$ peak in Figure 2a), the adsorption of pABA is studied only on the stoichiometric anatase (101) surface.

The structures studied in the DFT calculations are shown in Figure 5, and the adsorption energies are collected in Table 1. Eighteen starting structures were considered, but only 13 optimized structures were obtained (Supporting Information). The energies in Table 1 show that the structures adsorbed via only the carboxylic group are always more stable (typical adsorption energies of −1.0 to −0.8 eV) than those where the amino group is also adsorbed (adsorption energies of −0.5 eV and weaker). The exception is the zwitterion, which is very unfavorable in terms of the adsorption energy.

Among the structures that contain an adsorbed amino group, the structures with the nondissociated $NH_2$ group are relatively more stable, while the structures involving a dissociated NH group have positive adsorption energies, implying that these structures are less favorable than even a desorbed pABA molecule (but desorption does not take place in the calculation because of the high energy barrier required to break these Ti−N bonds). Nevertheless, even the most stable configurations containing an adsorbed amino group are still considerably less stable than the structures that are adsorbed only via the carboxylic group and are therefore unlikely to exist. This adsorption via the carboxylic group but not via the amino group agrees very well with the NEXAFS and photoelectron spectroscopy results.

Of the structures adsorbed only via the carboxylic group, nondissociatively adsorbed structures have slightly larger (by ∼0.1 eV) adsorption energies than dissociatively adsorbed structures. This is in agreement with earlier theoretical studies of carboxylic acid adsorption on anatase (101),[25−27] which show that molecular adsorption is energetically favored. However, these results are in contradiction with the photoelectron spectra, which clearly show that the pABA molecule is adsorbed dissociatively—both oxygens of the molecule have the same environment. This contradiction can be explained if we consider the possibility of the full monolayer coverage of the surface by the adsorbate. If the pABA molecule is adsorbed dissociatively, then at full monolayer coverage the shortest distance between atoms in neighboring molecules is approximately 3.6 Å, i.e., there is no steric clash (Figure 6a). However, if the molecules in the nondissociative configuration (optimized geometries d and e in Figure 5) are placed on this surface to achieve full coverage, then the shortest intermolecular distance can be as short as 0.6 Å (Figure 6b); this clearly leads to a very strained structure. This steric clash can be avoided if the adsorbate covers every other row of five-coordinated Ti atoms in the [010] direction rather than every row, but this arrangement would leave under-coordinated Ti atoms free to react with other pABA molecules that can adsorb in the dissociative configuration. Therefore, even if dissociative adsorption is slightly less energetically favorable for single adsorbed molecules, it is preferable because it allows full coverage of the anatase (101) surface with the pABA adsorbate.

The calculated adsorption geometry can be compared to the information on the molecular orientation given by angle-resolved NEXAFS measurements. The plane of the aromatic ring in the dissociated adsorption configuration (structure a in Figure 5) is tilted by 65.1° with respect to the surface (or 24.9° with respect to the surface normal). The plane of the ring is also twisted by 12.7° with respect to the [010] direction. These parameters are in excellent agreement with the angle-resolved NEXAFS results (tilt 60 ± 15° from the surface and twist angle of 7 ± 15° relative to the [010] azimuth). Structure b in Figure 5 also is compatible with experimental measurements (calculated tilt angle 52.7° and twist angle 13.9°), whereas the orientations of molecularly adsorbed structures d and e, where the molecule is approximately along the [$\bar{1}$01] direction, are not compatible with the NEXAFS results. The adsorption geometry of the zwitterion (tilt angle 5.6°, twist angle 1.1°, Figure 5c) is very different from the adsorption geometry of the dissociated molecule and also very different from the experimentally determined parameters: these results confirm that the adsorbed zwitterion is not formed in the experiment.


dx.doi.org/10.1021/la5032619 | Langmuir 2014, 30, 12306−12314

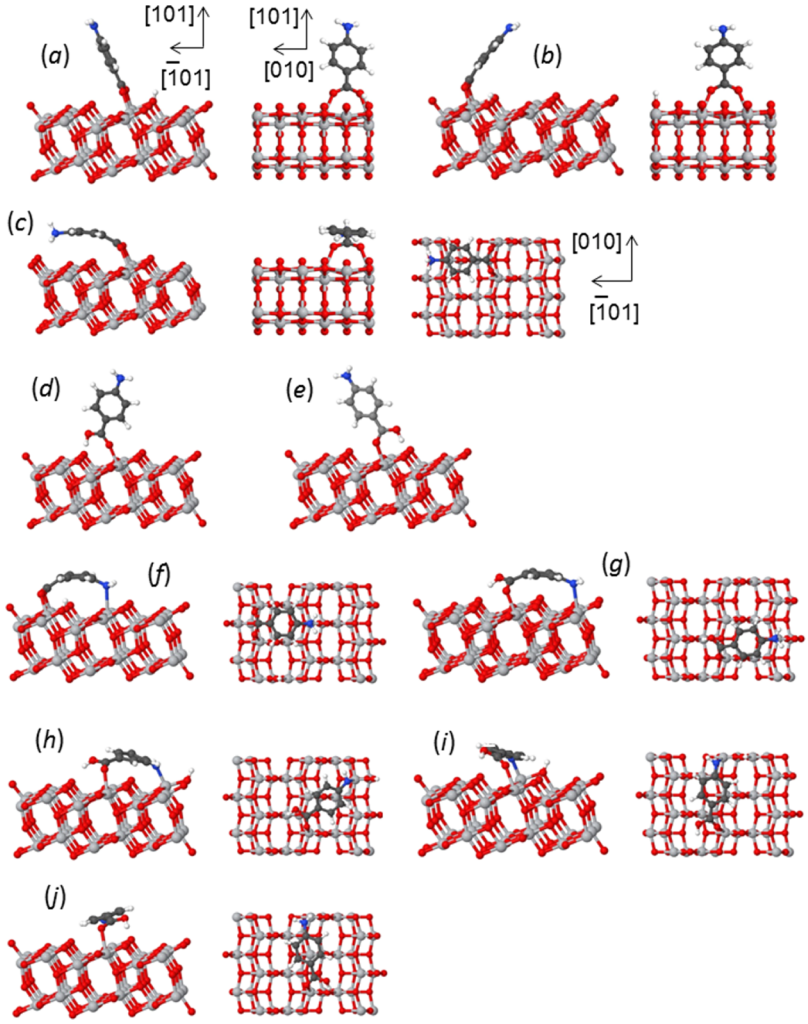


**Figure 5.** Adsorption configurations of pABA on anatase (101) obtained from DFT calculations: (a, b) dissociative adsorption of the carboxylic group, (c) dissociative adsorption of the carboxylic group of the zwitterion, (d, e) nondissociative adsorption of the carboxylic group (the carboxylic group is either above the surface trough or above the surface Ti−O bond), (f) dissociative adsorption of the carboxylic group and nondissociative adsorption of the amino group, (g−j) nondissociative adsorption of the carboxylic group and adsorption of the amino group. Structures f, g, and j can have the amino group adsorbed nondissociatively (as shown) or dissociatively; these latter structures have higher energies (Table 1) and are not shown in the figure. Red spheres represent oxygen, black is carbon, dark gray is titanium, blue is nitrogen, and light gray is hydrogen.

**Table 1. Adsorption Energies of pABA on Anatase (101)**

| label | adsorption mode of carboxylic group | adsorption mode of amino group | adsorption energy, eV |
|---|---|---|---|
| *a* | dissoc. | | −0.80 |
| *b* | dissoc. | | −0.24 |
| *c* | dissoc. (zwitterion) | | 0.53 |
| *d* | nondissoc. | | −0.96 |
| *e* | nondissoc. | | −0.93 |
| *f* | dissoc. | nondissoc. | 0.19 |
| *f′* | dissoc. | dissoc. | 1.75 |
| *g* | nondissoc. | nondissoc. | −0.42 |
| *g′* | nondissoc. | dissoc. | 0.70 |
| *h* | nondissoc. | dissoc. | 1.00 |
| *i* | nondissoc. | dissoc. | 0.82 |
| *j* | nondissoc. | nondissoc. | −0.47 |
| *j′* | nondissoc. | dissoc. | 0.88 |

**3.4. Occupied and Unoccupied Density of States Calculations and Valence Band Photoemission Spectroscopy.** The density of states (DOS) has been calculated for the dissociated (deprotonated) configuration to obtain additional information on the composition of the valence and conduction bands. Figure 7 shows that the calculated $TiO_2$ band gap is approximately 3.6 eV (slightly overestimated because of the use of the B3LYP functional); the HOMO of pABA lies approximately 1.3 eV above the top of the $TiO_2$ valence band and has the same energy both in the adsorbed and unbound pABA molecules. States near the bottom of the conduction band have a noticeable contribution of pABA orbitals (mainly from the oxygens and the carboxylate carbon, C7): these mixed states have no equivalent in the isolated pABA molecule whose LUMO can be seen as a sharp peak ∼2.5 eV above the conduction band minimum. Therefore, in the surface-adsorbate system, the lowest-energy excitation (and optical absorption) is likely to go from the pABA HOMO to the states at the bottom of the conduction band, which have mixed $TiO_2$-pABA character. The energy difference between these states and therefore the energy of this transition is approximately 2.3 eV according to the computational results. Bearing in mind that the $TiO_2$ band gap was overestimated by ∼0.4 eV in the calculations, this energy of 2.3 eV is also likely to


dx.doi.org/10.1021/la5032619 | *Langmuir* 2014, 30, 12306−12314

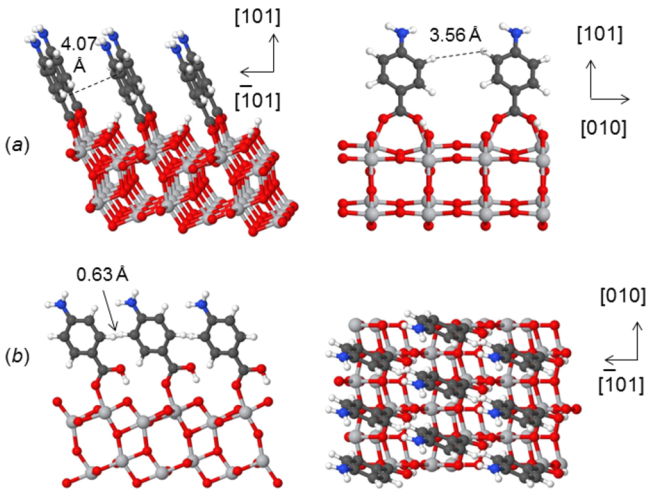


**Figure 6.** Models of adsorption geometries of pABA on anatase (101) at full coverage: (a) dissociative adsorption (two side views) and (b) nondissociative adsorption (side and top view). See Figure 5 for the key to the colors used.

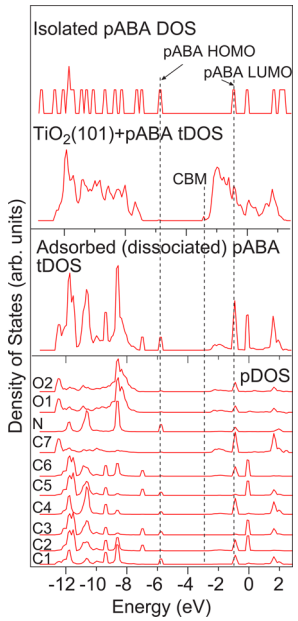


**Figure 7.** Total DOS (tDOS) and the contribution from individual pABA atoms (pDOS). Upper panel: total DOS for the substrate and adsorbate (scaled by the number of Ti atoms: 36 Ti atoms in the cell) and the DOS of an unbound pABA molecule. Middle panel: the contribution of the adsorbed pABA to the total DOS. Lower panel: individual atom contributions to the adsorbed pABA DOS. The HOMO and LUMO of the isolated pABA molecule and the conduction band minimum (CBM) of the $TiO_2$-adsorbate system are labeled. The vacuum level is set as the zero of energy.

be overestimated, and the energy of this transition is likely to be on the order of 1.9 eV, similar to the experimental UV−vis absorption of a pABA-$TiO_2$ nanoparticle complex (Supporting Information Figure S1).

The partial density of states in Figure 7 shows that the carboxylate carbon atom, C7, contributes to the state resulting from adsorption in the unoccupied DOS at around −2 eV with respect to the vacuum level. The two oxygen atoms also make a small contribution to this region of the unoccupied DOS. The presence of C7 states in this region may appear at odds with the StoBe-calculated NEXAFS spectra. However, it should be remembered that the NEXAFS calculations are for the excited state and account for the chemically shifted carboxylate C 1s from which the electron is excited as well as the unoccupied state into which it is excited.

Figure 8 shows valence band spectra recorded from clean anatase $TiO_2(101)$ ($h\nu$ = 40 eV) and anatase $TiO_2(101)$

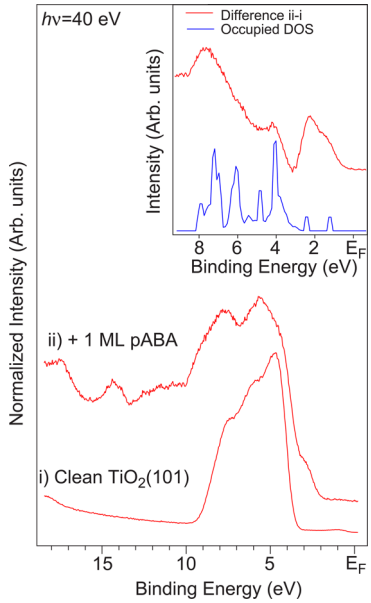


**Figure 8.** Valence band spectra recorded at a photon energy of 40 eV from the clean anatase $TiO_2$ surface, and the same surface following the adsorption of 1 ML pABA. The inset shows a portion of the difference spectrum obtained by subtracting the clean surface spectrum from that of the dosed one compared to the DFT calculated occupied density of states of the adsorbed pABA molecule.

following the adsorption of 1 ML pABA ($h\nu$ = 40 eV). The spectrum recorded from the clean anatase $TiO_2(101)$ surface is in good agreement with published valence band spectra recorded from this surface and at this photon energy.[19] The most obvious effect of adsorbing pABA onto $TiO_2$ is the location of the molecular HOMO density of states extending from the low-binding-energy side of the $TiO_2$ valence band to around 1.8 eV binding energy. Molecule-derived states in the band gap region have also been observed following catechol adsorption on this surface.[49] Other features due to the adsorption of the molecule are also apparent in the loss of structure in the valence band and in the appearance of new peaks at 9.4, 13.3, and 17.2 eV. The inset in Figure 8 shows a difference spectrum (obtained by normalizing the clean and dosed spectra to the background and then subtracting the clean spectrum from the dosed one) compared to the DFT calculated occupied DOS of the adsorbed pABA molecule. The DOS calculation was placed on the binding-energy scale by aligning the peaks at 5.8 and 6.9 eV in the calculation to the broad peak between 0 and 2 eV in the experimental valence band spectrum. We chose this as the normalization point because we expect the highest occupied molecular orbitals (HOMOs) to be associated mainly with the ring $\pi$ system and therefore less likely to be perturbed by bonding to the surface. The large dip in the difference spectrum at 4.6 eV is an artifact of the subtraction process. The agreement between the calculated DOS and experimental data is rather good, although the molecular


dx.doi.org/10.1021/la5032619 | Langmuir 2014, 30, 12306−12314

HOMO-derived peaks are much narrower than the experimentally derived peaks.

In summary, the valence band spectra and DOS calculations suggest that it is the position of the HOMO (ring $\pi$-bonding)-derived states coupled with the presence of new molecular states in the adsorbed molecule that leads to the reduction in the optical band gap observed in the UV−vis spectrum. The highest occupied molecular orbital to lowest unoccupied molecular orbital (HOMO−LUMO) excitation energy in the free pABA molecule is 3.4 eV. For catechol and dopamine on $TiO_2$, it was suggested that the adsorption of the molecule to $TiO_2$ leads to the presence of new molecule−substrate-derived states close to the bottom of the conduction band of the $TiO_2$.[18,34] This leads to the observed change in the optical absorption onset in catechol-$TiO_2$ nanoparticle complexes. The DOS calculations for the adsorbed molecule support a similar process leading to the formation of the yellow pABA-$TiO_2$ nanoparticle "complex". This yellow-colored complex was also observed in the work of Rahal et al.[13] It is well known that the *p*-aminobenzoate ion is also yellow, which strongly suggests that the color change on adsorption is linked to electronic structure changes upon ionization of the molecule. We propose that it is these changes and the formation of new molecule−substrate-derived states that lead to the change in optical absorption of the pABA-$TiO_2$ nanoparticle complex rather than a direct molecule-to-$TiO_2$ conduction band transfer process.

## 4. CONCLUSIONS

*p*-Aminobenzoic acid was found to adsorb on the $TiO_2$(101) anatase surface in a bidentate mode, most likely bridging neighboring 5-fold-coordinated Ti atoms in the [010] direction. Core-level spectra suggest that the molecule adsorbs following deprotonation of the carboxyl group and the zwitterion is not formed upon adsorption. This is supported by the DFT calculations of adsorption energies, which find zwitterion formation to be particularly unstable. The amine group appears to remain intact and oriented away from the surface at monolayer coverage and could therefore be available for the grafting of biomolecules or light-harvesting quantum dots. Angle-resolved NEXAFS spectra and DFT-derived adsorption structures indicate the ring of the molecule to be tilted at 30 ± 5° with respect to the surface normal and twisted relative to the [010] azimuth. The observed shift in the optical absorption spectrum of the pABA-functionalized $TiO_2$ is attributed to excitations between the molecular HOMO and the presence of new molecular states, resulting from the deprotonation of the adsorbed carboxyl group, close to the foot of the $TiO_2$ conduction band.

## ■ ASSOCIATED CONTENT

### Supporting Information

UV−vis absorption onset. DFT calculations: bonding mode and orientation. This material is available free of charge via the Internet at http://pubs.acs.org.

## ■ AUTHOR INFORMATION


### Present Address

(A.L.) Sorbonne Universités, UPMC, Paris 06, CNRS, INSP, UMR 7588, F-75252, Paris Cedex 05, France.


### Notes

The authors declare no competing financial interest.

## ■ ACKNOWLEDGMENTS


We thank Synchrotron Soleil, MAX-lab, and the CALIPSO project funded by the European Commission under the Seventh Framework Programme for the beam time award. M.J.J. thanks EPSRC for the award of a studentship under the NowNano Doctoral Training Centre (grant EP/G03737X/1). M.W. and H.R. thank EPSRC for studentships and The University of Manchester for president's scholarships. A.G.T. thanks The Photon Science Institute and The University of Manchester for additional funding. We also thank Alexei Preobrajenski for assistance with the D1011 beamline.


## ■ REFERENCES


(1) O' Regan, B.; Grätzel, M. A Low-Cost, High-Efficiency Solar-Cell Based on Dye-Sensitized Colloidal $TiO_2$ Films. *Nature* **1991**, *353*, 737−740.

(2) Xie, Q.; Zhao, Y. Y.; Chen, X.; Liu, H. M.; Evans, D. G.; Yang, W. S. Nanosheet-based titania microspheres with hollow core-shell structure encapsulating horseradish peroxidase for a mediator-free biosensor. *Biomaterials* **2011**, *32*, 6588−6594.

(3) Diebold, U. The surface science of titanium dioxide. *Surf. Sci. Rep.* **2003**, *48*, 53−229.

(4) Pang, C. L.; Lindsay, R.; Thornton, G. Chemical reactions on rutile $TiO_2$(110). *Chem. Soc. Rev.* **2008**, *37*, 2328−2353.

(5) Jones, F. H. Teeth and bones: applications of surface science to dental materials and related biomaterials. *Surf. Sci. Rep.* **2001**, *42*, 79−205.

(6) Fleming, G. J.; Adib, K.; Rodriguez, J. A.; Barteau, M. A.; Idriss, H. Proline adsorption on $TiO_2$(110) single crystal surface: A study by high resolution photoelectron spectroscopy. *Surf. Sci.* **2007**, *601*, 5726−5731.

(7) Tonner, R. Adsorption of Proline and Glycine on the $TiO_2$(110) Surface: A Density Functional Theory Study. *ChemPhysChem* **2010**, *11*, 1053−1061.

(8) Wilson, J. N.; Dowler, R. M.; Idriss, H. Adsorption and reaction of glycine on the rutile $TiO_2$(011) single crystal surface. *Surf. Sci.* **2011**, *605*, 206−213.

(9) Rajh, T.; Saponjic, Z.; Liu, J. Q.; Dimitrijevic, N. M.; Scherer, N. F.; Vega-Arroyo, M.; Zapol, P.; Curtiss, L. A.; Thurnauer, M. C. Charge transfer across the nanocrystalline-DNA interface: Probing DNA recognition. *Nano Lett.* **2004**, *4*, 1017−1023.

(10) Kotsokechagia, T.; Zaki, N. M.; Syres, K.; de Leonardis, P.; Thomas, A.; Cellesi, F.; Tirelli, N. PEGylation of Nanosubstrates (Titania) with Multifunctional Reagents: At the Crossroads between Nanoparticles and Nanocomposites. *Langmuir* **2012**, *28*, 11490−11501.

(11) Mora-Sero, I.; Gimenez, S.; Moehl, T.; Fabregat-Santiago, F.; Lana-Villareal, T.; Gomez, R.; Bisquert, J. Factors determining the photovoltaic performance of a CdSe quantum dot sensitized solar cell: the role of the linker molecule and of the counter electrode. *Nanotechnology* **2008**, *19*, 424007.

(12) Robel, I.; Subramanian, V.; Kuno, M.; Kamat, P. V. Quantum Dot Solar Cells. Harvesting Light Energy with CdSe Nanocrystals Molecularly Linked to Mesoscopic $TiO_2$ Films. *J. Am. Chem. Soc.* **2006**, *128*, 2385−2393.

(13) Rahal, R.; Daniele, S.; Hubert-Pfalzgraf, L. G.; Guyot-Ferréol, V.; Tranchant, J.-F. Synthesis of para-Amino Benzoic Acid−TiO2 Hybrid Nanostructures of Controlled Functionality by an Aqueous One-Step Process. *Eur. J. Inorg. Chem.* **2008**, *2008*, 980−987.

(14) Rahal, R.; Daniele, S.; Jobic, H. Inelastic neutron scattering study of the coordination of para-amino benzoic acid molecules to the surface of nanocrystalline titania particles. *Chem. Phys. Lett.* **2009**, *472*, 65−68.

(15) Persson, P.; Bergstrom, R.; Lunell, S. Quantum chemical study of photoinjection processes in dye-sensitized $TiO_2$ nanoparticles. *J. Phys. Chem. B* **2000**, *104*, 10348−10351.

(16) Talrose, V.; Stern, E. B.; Goncharova, A. A.; Messineva, N. A.; Trusova, N. V.; Efimkina, M. V. UV/Visible Spectra. In *NIST Chemistry WebBook*; Linstrom, P. J., Mallard, W. G., Eds.; NIST Standard Reference Database Number 69; National Institute of Standards and Technology: Gaithersburg, MD; accessed July 2014.
(17) Lazzeri, M.; Vittadini, A.; Selloni, A. Structure and energetics of stoichiometric $TiO_2$ anatase surfaces. *Phys. Rev. B* **2001**, *63*, 155409.
(18) Syres, K.; Thomas, A.; Bondino, F.; Malvestuto, M.; Grätzel, M. Dopamine Adsorption on Anatase $TiO_2$(101): A Photoemission and NEXAFS Spectroscopy Study. *Langmuir* **2010**, *26*, 14548−14555.
(19) Thomas, A. G.; Flavell, W. R.; Mallick, A. K.; Kumarasinghe, A. R.; Tsoutsou, D.; Khan, N.; Chatwin, C.; Rayner, S.; Smith, G. C.; Stockbauer, R. L.; et al. Comparison of the electronic structure of anatase and rutile $TiO_2$ single-crystal surfaces using resonant photoemission and X-ray absorption spectroscopy. *Phys. Rev. B* **2007**, *75*, 035105.
(20) Dovesi, R.; Orlando, R.; Civalleri, B.; Roetti, C.; Saunders, V. R.; Zicovich-Wilson, C. M. CRYSTAL: a computational tool for the ab initio study of the electronic properties of crystals. *Z. Kristallogr.* **2005**, *220*, 571−573.
(21) Dovesi, R.; Saunders, V. R.; Roetti, C.; Orlando, R.; Zicovich-Wilson, C. M.; Pascale, F.; Civalleri, B.; Doll, K.; Harrison, N. M.; Bush, I. J., et al. *CRYSTAL09 User's Manual*; University of Torino: Turin, Italy, 2009.
(22) http://www.crystal.unito.it/Basis_Sets/Ptable.html. Last Accessed July 7, 2014.
(23) Becke, A. D. Density-functional exchange-energy approximation with correct asymptotic behavior. *Phys. Rev. A* **1988**, *38*, 3098−3100.
(24) Lee, C.; Yang, W.; Parr, R. G. Development of the Colle-Salvetti correlation-energy formula into a functional of the electron density. *Phys. Rev. B* **1988**, *37*, 785−789.
(25) Martsinovich, N.; Jones, D. R.; Troisi, A. Electronic Structure of $TiO_2$ Surfaces and Effect of Molecular Adsorbates Using Different DFT Implementations. *J. Phys. Chem. C* **2010**, *114*, 22659−22670.
(26) Martsinovich, N.; Troisi, A. How $TiO_2$ crystallographic surfaces influence charge injection rates from a chemisorbed dye sensitiser. *Phys. Chem. Chem. Phys.* **2012**, *14*, 13392−13401.
(27) Vittadini, A.; Selloni, A.; Rotzinger, F. P.; Grätzel, M. Formic Acid Adsorption on Dry and Hydrated $TiO_2$ Anatase (101) Surfaces by DFT Calculations. *J. Phys. Chem. B* **2000**, *104*, 1300−1306.
(28) Boys, S. F.; Bernardi, F. The calculation of small molecular interactions by the differences of separate total energies. Some procedures with reduced errors. *Mol. Phys.* **1970**, *19*, 553−566.
(29) Frisch, M. J.; Trucks, G. W.; Schlegel, H. B.; Scuseria, G. E.; Robb, M. A.; Cheeseman, J. R.; Montgomery, J. A.; Vreven, T.; Kudin, K. N.; Burant, J. C., et al. *Gaussian 03* , Revision B.04; Gaussian, Inc.: Wallingford, CT, 2004.
(30) Hermann, K.; Pettersson, L. *StoBe-deMon* Software, Stockholm-Berlin version 2.2 of deMon, 2006.
(31) Schnadt, J.; O'Shea, J. N.; Patthey, L.; Schiessling, J.; Krempasky, J.; Shi, M.; Mårtensson, N.; Bruhwiler, P. A. Structural study of adsorption of isonicotinic acid and related molecules on rutile $TiO_2$(110) II: XPS. *Surf. Sci.* **2003**, *544*, 74−86.
(32) He, Y. B.; Dulub, O.; Cheng, H. Z.; Selloni, A.; Diebold, U. Evidence for the Predominance of Subsurface Defects on Reduced Anatase $TiO_2$(101). *Phys. Rev. Lett.* **2009**, *102*, 4.
(33) Setvin, M.; Hao, X.; Daniel, B.; Pavelec, J.; Novotny, Z.; Parkinson, G. S.; Schmid, M.; Kresse, G.; Franchini, C.; Diebold, U. Charge Trapping at the Step Edges of $TiO_2$ Anatase (101). *Angew. Chem., Int. Ed.* **2014**, *53*, 4714−4716.
(34) Syres, K. L.; Thomas, A. G.; Flavell, W. R.; Spencer, B. F.; Bondino, F.; Malvestuto, M.; Preobrajenski, A.; Graetzel, M. Adsorbate-Induced Modification of Surface Electronic Structure: Pyrocatechol Adsorption on the Anatase $TiO_2$ (101) and Rutile $TiO_2$ (110) Surfaces. *J. Phys. Chem. C* **2012**, *116*, 23515−23525.
(35) Thomas, A. G.; Jackman, M. J.; Syres, K. L.; Wagstaffe, M.; Li, T.-L.; Schlueter, C. Depth profiling of the band gap state in anatase $TiO_2$(101). To be submitted for publication.
(36) Lu, G.; Bernasek, S. L.; Schwartz, J. Oxidation of a polycrystalline titanium surface by oxygen and water. *Surf. Sci.* **2000**, *458*, 80−90.
(37) Blomquist, J.; Walle, L. E.; Uvdal, P.; Borg, A.; Sandell, A. Water Dissociation on Single Crystalline Anatase $TiO_2$(001) Studied by Photoelectron Spectroscopy. *J. Phys. Chem. C* **2008**, *112*, 16616−16621.
(38) O'Shea, J. N.; Luo, Y.; Schnadt, J.; Patthey, L.; Hillesheimer, H.; Krempasky, J.; Nordlund, D.; Nagasono, M.; Bruhwiler, P. A.; Martensson, N. Hydrogen-bond induced surface core-level shift in pyridine carboxylic acids. *Surf. Sci.* **2001**, *486*, 157−166.
(39) Patthey, L.; Rensmo, H.; Persson, P.; Westermark, K.; Vayssieres, L.; Stashans, A.; Petersson, A.; Bruhwiler, P. A.; Siegbahn, H.; Lunell, S.; et al. Adsorption of bi-isonicotinic acid on rutile $TiO_2$(110). *J. Chem. Phys.* **1999**, *110*, 5913−5918.
(40) Thomas, A.; Syres, K. Adsorption of organic molecules on rutile $TiO_2$ and anatase $TiO_2$ single crystal surfaces. *Chem. Soc. Rev.* **2012**, *41*, 4207−4217.
(41) O'Shea, J. N.; Schnadt, J.; Bruhwiler, P. A.; Hillesheimer, H.; Martensson, N.; Patthey, L.; Krempasky, J.; Wang, C. K.; Luo, Y.; Agren, H. Hydrogen-bond induced surface core-level shift in isonicotinic acid. *J. Phys. Chem. B* **2001**, *105*, 1917−1920.
(42) Woodruff, D. P. Angular dependence in photoemission: from atoms to surfaces to atoms. *J. Electron Spectrosc. Relat. Phenom.* **1999**, *100*, 259−272.
(43) Lopez, A.; Bitzer, T.; Heller, T.; Richardson, N. V. Functional group selectivity in adsorption of 4-aminobenzoic acid on clean and Na modified Si(100)-2 × 1 surfaces. *Surf. Sci.* **2001**, *480*, 65−72.
(44) Gutierrez-Sosa, A.; Martinez-Escolano, P.; Raza, H.; Lindsay, R.; Wincott, P. L.; Thornton, G. Orientation of carboxylates on $TiO_2$(110). *Surf. Sci.* **2001**, *471*, 163−169.
(45) Stöhr, J. *NEXAFS Spectroscopy*; Springer-Verlag: Berlin, 2003.
(46) Guo, Y.-n.; Lu, X.; Zhang, H.-p.; Weng, J.; Watari, F.; Leng, Y. DFT Study of the Adsorption of Aspartic Acid on Pure, N-Doped, and Ca-Doped Rutile (110) Surfaces. *J. Phys. Chem. C* **2011**, *115*, 18572−18581.
(47) Li, C.; Monti, S.; Carravetta, V. Journey toward the Surface: How Glycine Adsorbs on Titania in Water Solution. *J. Phys. Chem. C* **2012**, *116*, 18318−18326.
(48) Szieberth, D.; Maria Ferrari, A.; Dong, X. Adsorption of glycine on the anatase (101) surface: an ab initio study. *Phys. Chem. Chem. Phys.* **2010**, *12*, 11033−11040.
(49) Li, S. C.; Wang, J. G.; Jacobson, P.; Gong, X. Q.; Selloni, A.; Diebold, U. Correlation between Bonding Geometry and Band Gap States at Organic-Inorganic Interfaces: Catechol on Rutile $TiO_2$(110). *J. Am. Chem. Soc.* **2009**, *131*, 980−984.